

Ozone hole and Southern Hemisphere climate change

Seok-Woo Son,¹ Neil F. Tandon,² Lorenzo M. Polvani,³ and Darryn W. Waugh⁴

Received 16 April 2009; revised 28 June 2009; accepted 13 July 2009; published 11 August 2009.

[1] Climate change in the Southern Hemisphere (SH) has been robustly documented in the last several years. It has altered the atmospheric circulation in a surprising number of ways: a rising global tropopause, a poleward intensification of the westerly jet, a poleward shift in storm tracks, a poleward expansion of the Hadley cell, and many others. While these changes have been extensively related with anthropogenic warming resulting from the increase in greenhouse gases, their potential link to stratospheric cooling resulting from ozone depletion has only recently been examined and a comprehensive picture is still lacking. Examining model output from the coupled climate models participating in the Intergovernmental Panel on Climate Change (IPCC) Fourth Assessment (AR4), and grouping them depending on the stratospheric ozone forcing used, we here show that stratospheric ozone affects the entire atmospheric circulation in the SH, from the polar regions to the subtropics, and from the stratosphere to the surface. Furthermore, model projections suggest that the anticipated ozone recovery, resulting from the implementation of the Montreal Protocol, will likely decelerate future climate change resulting from increased greenhouse gases, although it might accelerate surface warming over Antarctica.

Citation: Son, S.-W., N. F. Tandon, L. M. Polvani, and D. W. Waugh (2009), Ozone hole and Southern Hemisphere climate change, *Geophys. Res. Lett.*, 36, L15705, doi:10.1029/2009GL038671.

[2] Recent studies have shown that, in the late 20th century, depletion of stratospheric ozone by anthropogenic halogen compounds has affected the SH surface climate by forcing sea-level-pressure (SLP) to decrease in high latitudes and to increase in mid latitudes [Thompson and Solomon, 2002; Marshall, 2003]. This dipolar SLP change, which is robustly found in climate model integrations [Gillett and Thompson, 2003; Shindell and Schmidt, 2004; Miller *et al.*, 2006; Arblaster and Meehl, 2006; Cai and Cowan, 2007], is qualitatively similar to the so-called Southern Annular Mode (SAM) [Thompson *et al.*, 2000], and intimately related to the latitudinal position of the midlatitude jet [Thompson *et al.*, 2000; Son *et al.*, 2008]. While this suggests that stratospheric ozone plays an

important role in controlling tropospheric circulation [e.g., Gillett and Thompson, 2003], its detailed impact on the various components of the SH climate system, from the polar regions to the subtropics, remains unclear at present. This question is especially pertinent in view of the predicted recovery of stratospheric ozone [e.g., Eyring *et al.*, 2007] which, as a result of the implementation of the Montreal Protocol, is expected to occur in the next 50–60 years.

[3] In this study, we demonstrate the pervasive impacts of stratospheric ozone on SH climate change by examining output from the IPCC/AR4 models [Meehl *et al.*, 2007]. Both past (20C3M) and future scenario integrations with moderate greenhouse-gas forcing (A1B) are analyzed, ozone forcing being the key discriminating factor among the models. As indicated in Table 1, not all IPCC/AR4 models included ozone depletion and recovery [Miller *et al.*, 2006; Cai and Cowan, 2007; Karpechko *et al.*, 2008; Son *et al.*, 2008]. Of the 20 models used in this study, roughly half used ozone depletion or recovery; others simply use monthly climatological ozone fields, which do not change from year to year. Since the rates of ozone depletion and recovery vary among the models, and since actual ozone fields used were not archived, a detailed intermodel comparison is not possible. We thus adopt the strategy of grouping the models into four sets: those with and without ozone depletion in the past, and those with and without ozone recovery in the future. This simple multimodel averaging scheme reveals a remarkably consistent impact of stratospheric ozone on the various components of the SH climate system. It should be noted that comparison among these four sets of models may not be a fair comparison, as each model set comprises very different models. This comparison, however, is made by assuming that the trend difference caused by different external forcings (e.g., ozone depletion vs. recovery) is larger than the one caused by model-dependent internal processes. Although this is a quite strong assumption, it seems to hold, as shown below.

[4] The results of our analysis are summarized in Figure 1. In all panels, the 4 symbols with error bars show the multimodel mean trend, plus/minus one standard deviation, of models with and without ozone depletion (red and green circles, respectively), and without and with ozone recovery (green and blue squares, respectively). For all quantities, the linear trends are computed between 1960 and 1999 (for the past) and between 2000 and 2049 (for the future). These periods are chosen to capture the ozone depletion and recovery periods; note that only the first half of the 21st century is used since ozone recovery is expected to be strongest in that period [Eyring *et al.*, 2007]. Trends are first calculated from monthly-averaged fields for individual model realizations with a least-square fit, then averaged for all available ensemble members for each model, and finally averaged across all the models to construct the multimodel mean. Except for Figure 1a, all trends are shown for the

¹Department of Atmospheric and Oceanic Sciences, McGill University, Montreal, Quebec, Canada.

²Department of Applied Physics and Applied Mathematics, Columbia University, New York, New York, USA.

³Department of Applied Physics and Applied Mathematics and Department of Earth and Environmental Sciences, Columbia University, New York, New York, USA.

⁴Department of Earth and Planetary Sciences, Johns Hopkins University, Baltimore, Maryland, USA.

Table 1. IPCC/AR4 Models Used in This Study^a

Model Name	20C3M	A1B
CSIRO Mk3.0	2/3(Y)	1(Y)
GFDL CM2.0	3(Y)	1(Y)
GFDL CM2.1	3(Y)	1(Y)
INGV SXG	1(Y)	1(Y)
MIROC3.2(medres)	3(Y)	3(Y)
MPI ECHAM5/MPI-OM	4(Y)	4(Y)
NCAR CCSM3.0	8(Y)	7(Y)
NCAR PCM1	4(Y)	4(Y)
UKMO HadCM3	2(Y)	1(Y)
UKMO HadGEM1	2(Y)	1(Y)
GISS EH	5(Y)	3(N)
GISS ER	9(Y)	5/2(N)
BCCR BCM2.0	1(N)	1(N)
CCCma CGCM3.1(T63)	1(N)	1(N)
CNRM CM3 ^b	1(N)	1(N)
GISS AOM	2(N)	2(N)
IAP FGOALS-g1.0	3(N)	3(N)
INM CM3.0	1(N)	1(N)
IPSL CM4	2(N)	1(N)
MRI CGCM2.3.2	5(N)	5(N)

^aNumber and parenthesized symbol, respectively, denote number of ensemble members and presence of time-varying stratospheric ozone in each model. If number of ensemble members are different for free atmosphere (former) and surface variables (latter number), they are indicated separately.

^bDocumentation claims inclusion of time-varying stratospheric ozone. However, Antarctic polar-cap temperature does not show the ozone impact in both the 20C3M and A1B scenario integrations [e.g., see *Son et al.*, 2008, Figure 3c].

December–February (DJF) period, i.e., SH summer. It has been shown that, although stratospheric ozone has a maximum trend in late spring, its impact on the surface climate is delayed and reaches a maximum in summer [*Thompson and Solomon*, 2002; *Son et al.*, 2008].

[5] Consider first how stratospheric ozone affects lower stratospheric temperatures in the southern high latitudes. Figure 1a shows polar-cap temperature trends, at 100 hPa, integrated south of 70°S, during October–January (ONDJ). In the absence of ozone depletion and recovery (green) polar-cap temperature shows very weak cooling trends, in both the past and scenario integrations. In contrast, strong cooling accompanies ozone depletion (red) and warming accompanies ozone recovery (blue), as expected from a direct ozone-induced radiative effect. Notice that the cooling rate associated with ozone depletion is somewhat stronger than the warming rate associated with ozone recovery. This asymmetry is consistent with the observed and predicted ozone trends [*Eyring et al.*, 2007], i.e., a relatively rapid depletion followed by a slower recovery. Such asymmetry, however, is not found in the SH winter (Figure S1a of the auxiliary material) or the NH (Figures S4a and S4c); temperature trends are rather similar in all data sets, as expected, since ozone trends are negligible for these regions and seasons.¹ This is strong evidence suggesting that differences between model sets in Figure 1a are primarily due to differences in stratospheric ozone. Notice also that the multimodel mean cooling rate, -2.0 K/decade, is comparable to the observed value of -1.9 K/decade between 1969 and 1996 around 65°–75°S [*Thompson and Solomon*, 2002; *Karpechko et al.*, 2008]. It indicates that the

IPCC/AR4 models are capable of simulating the observed temperature changes in the lower stratosphere, if the trends in ozone are prescribed.

[6] The lower-stratospheric temperature trends directly affect the height of the extratropical tropopause, defined by a temperature lapse rate equal to 2 K/km, as shown in Figure 1b. Due to ozone-induced stratospheric cooling, the SH extratropical tropopause height (pressure) has rapidly been increasing (decreasing) in the recent past [*Son et al.*, 2009]. This trend is well captured by models with prescribed ozone depletion (red), but severely underestimated in its absence (green). The multimodel mean further suggests that, accompanying ozone recovery, tropopause height trends might change sign in the future (blue).

[7] These systematic trends in tropopause height associated with ozone changes have important implications for the tropospheric circulation. Idealized models have shown that lowering the tropopause pressure, e.g., owing to stratospheric cooling, robustly induces a poleward shift in midlatitude jet [*Polvani and Kushner*, 2002; *Lorenz and DeWeaver*, 2007]. The IPCC/AR4 models show this as well, as can be seen in Figure 1c [see also *Lorenz and DeWeaver*, 2007]. The westerly jet, whose location is identified by the location of the maximum zonal wind at 850 hPa, shifts poleward even in the absence of ozone depletion/recovery, and it can be attributed to greenhouse gas forcing. This poleward shift is then strengthened by ozone depletion and, conversely, weakened by ozone recovery. Note that this sensitivity is not found in the SH winter (Figures S1c and S2) or in the NH (Figures S4b and S4d). Again, it is to be expected since ozone trends are almost negligible for those regions and seasons.

[8] Accompanying the latitudinal shift of the westerly jet, the IPCC/AR4 models show that ozone changes affect the location of poleward boundary of the Hadley cell, identified by zero value of 500-hPa mass stream function [e.g., *Hu and Fu*, 2007]. As can be seen in Figure 1d, ozone depletion tends to strengthen the expansion of the Hadley cell, while ozone recovery tends to weaken it. Although the error bar is relatively large and the trend difference between model sets with and without ozone depletion (or recovery) is within one standard deviation, the systematic differences in the Hadley cell trends are well correlated with trends in the jet location shown in Figure 1c [see also *Lu et al.*, 2008].

[9] Figure 2 shows the relationships between the trend in jet location and trend in Hadley-cell boundary for the individual models. The models prescribing ozone depletion (red circles) and recovery (blue squares) are remarkably well separated. There is no overlapping at all in jet trends, i.e., all 12 models prescribing ozone depletion show stronger negative trend than any models prescribing ozone recovery. For the Hadley-cell expansion, although few models prescribing ozone depletion show a comparable trend to the scenario integrations with ozone recovery, it is still clear that two sets of models are well separated. These results, along with the lack of systematic differences in the SH winter (Figures S1d and S2), suggest that stratospheric ozone plays a significant role in the SH subtropical circulation changes. It should be noted that the rate of expansion of the Hadley cell simulated by the IPCC/AR4 models (red circle in Figure 1d), about 0.6° for 4 decades, is much weaker than the one in satellite observations of about 1.2° in last 2 decades [*Hu and Fu*, 2007]. This indicates that

¹Auxiliary materials are available in the HTML. doi:10.1029/2009GL038671.

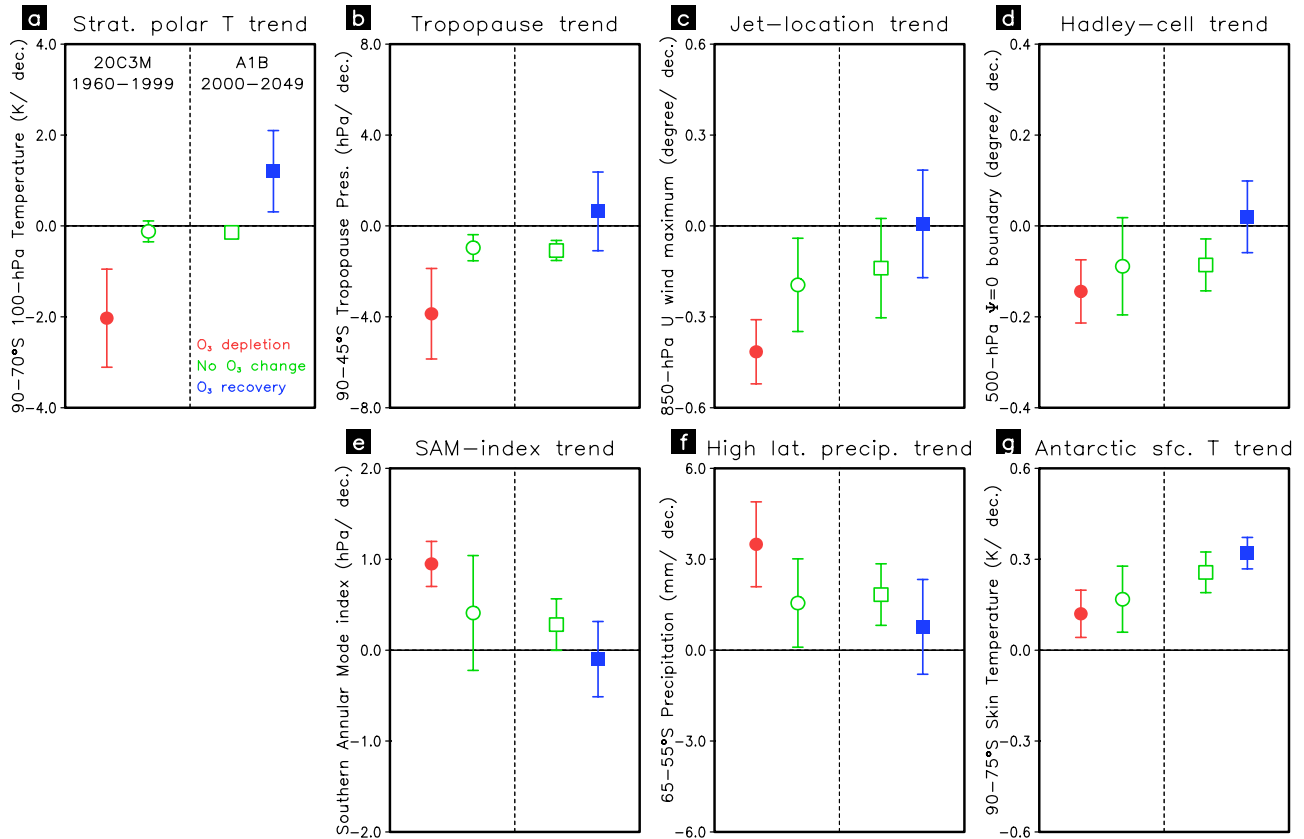


Figure 1. SH summer climate changes in four sets of the IPCC/AR4 models: The multimodel mean trends and one standard deviations are shown for (a) polar-cap temperature at 100 hPa, integrated south of 70°S with area weight, (b) tropopause pressure, integrated south of 45°S with area weight, (c) jet location as defined by the location of maximum zonal-mean zonal wind at 850 hPa, (d) the Hadley-cell boundary as defined by the location of zero mass stream function (ψ) at 500 hPa, (e) the SAM index as defined by sea level pressure difference between 40°S and 65°S, (f) precipitation, integrated from 65°S to 55°S with area weight, and (g) Antarctic skin temperature, integrated south of 75°S with area weight. All variables are shown for December–February except in Figure 1a where polar-cap temperature trends are shown for October–January. The negative values in Figure 1b denote a rise in tropopause height, and those in Figures 1c and 1d denote poleward shift in westerly jet and poleward expansion of the Hadley cell. The linear trends are computed for the time period of 1960–1999 in the 20C3M integrations (circles) and for the time period of 2000–2049 in the A1B scenario integrations (squares), and separately shown for models with (red, blue) and without time-varying stratospheric ozone (green).

coupled climate models underestimate the Hadley-cell expansion in the recent past.

[10] We next turn to surface climate. The long-term trends in extratropical SLP, precipitation and Antarctic skin temperature are presented in Figures 1e–1g, with the corresponding spatial patterns illustrated in Figure 3. For SLP (see Figure 1e), we compute the trend in the difference between 40°S and 65°S, which is equivalent to the SAM index [Marshall, 2003]. Consistent with previous studies [e.g., Gillett and Thompson, 2003; Shindell and Schmidt, 2004; Miller et al., 2006; Arblaster and Meehl, 2006; Cai and Cowan, 2007], and with the trends of the westerly jet (Figure 1c), ozone depletion has strengthened the positive trend of the SAM index caused by greenhouse-gas increase, making the dipolar change of SLP stronger than it would have been without it, as seen in Figure 3 (top). Note that the simulated trend of the SAM index, 0.9 hPa/decade (red dot in Figure 1e), is comparable to the observed trend of 1.0 hPa/decade between 1959 and 2000 [Marshall, 2003]. In

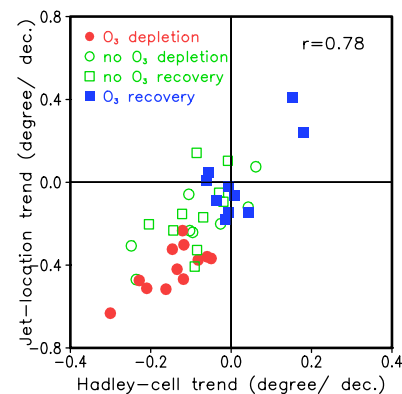


Figure 2. Trend relationship between the location of westerly jet and the poleward boundary of the Hadley cell in the SH summer. Color code is identical to one in Figure 1, and negative values denote the poleward shift of westerly jet and poleward expansion of the Hadley cell.

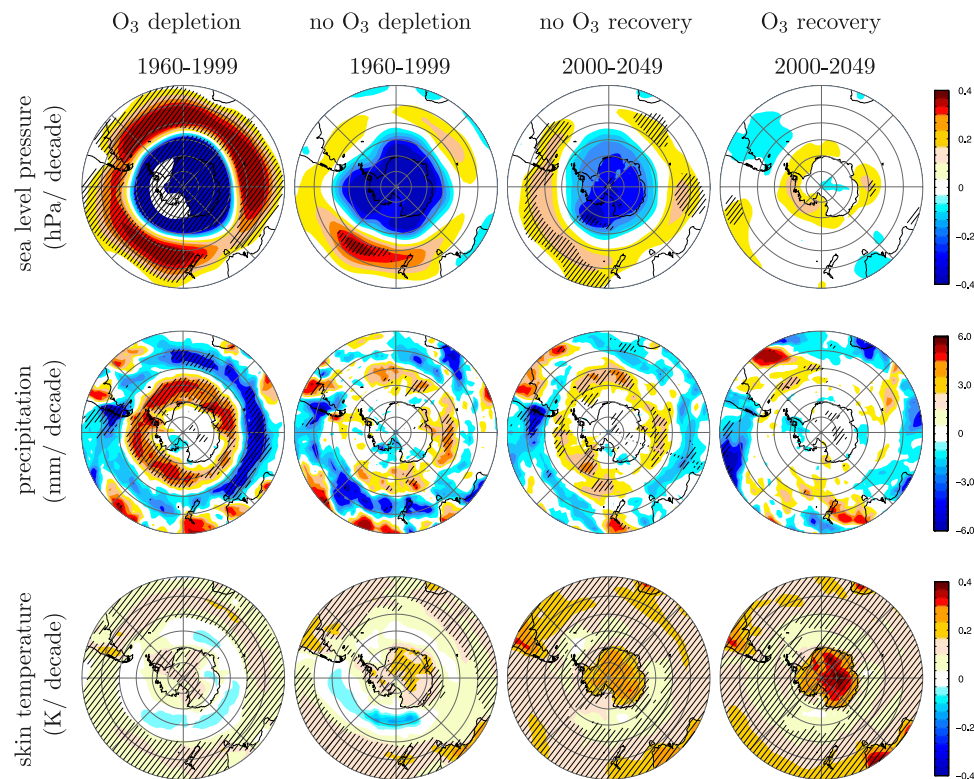


Figure 3. SH summer climate changes in four sets of the IPCC/AR4 models: The multimodel mean trends are shown for (top) sea level pressure, (middle) precipitation and (bottom) skin temperature. From left to right, trends are shown for models with and without ozone depletion in the past and those without and with ozone recovery in the future. In all fields, multimodel mean trends are calculated by linearly interpolating each model's trend to the specified grid points, and values greater than or equal to one standard deviation are hatched.

the presence of ozone recovery, however, the trend is predicted to be substantially weakened.

[11] The positive trend in the SAM index or the poleward shift in westerly jet are known to accompany a poleward shift in the storm tracks [Gillett and Thompson, 2003; Yin, 2005], which results in more precipitation in high latitudes and less precipitation in mid latitudes. This precipitation change is well captured in Figure 1f and Figure 3 (middle). Notice again how the projected ozone recovery is likely to reverse and possibly cancel the trends of the past few decades.

[12] Finally, sensitivity to stratospheric ozone is also found in Antarctic skin temperatures (Figure 1g). Ozone depletion appears to have weakened the greenhouse gas warming in the last several decades, and greater warming will accompany the expected ozone recovery (Figure 3, bottom). Although the models fail to reproduce the recent sharp warming over the Antarctic peninsula, the overall result is consistent with recent finding [Steig et al., 2009]. In order to validate these results, identical analyses were performed for surface climate in the SH winter; as expected, multimodel averages do show no systematic variation between model sets in that season (Figure S3).

[13] In sum, the IPCC/AR4 models show a broad and systematic impact of stratospheric ozone on the SH summer climate system. Ozone depletion has likely contributed to decreasing lower-stratospheric temperatures, increasing tropopause height, poleward shifting of the westerly jet in midlatitudes, expanding the Hadley cell poleward, increas-

ing high-latitude precipitation, and increasing the SAM index. In addition, model predictions indicate that these effects will likely be reversed by the ozone recovery in the next several decades.

[14] These results however are only qualitative since ozone data are not available and the number of models is limited. More quantitative studies, using larger number of models or multiple realizations with and without time-varying ozone in a same model, are needed to confirm and corroborate our findings.

[15] **Acknowledgments.** We thank the Program for Climate Model Diagnosis and Intercomparison (PCMDI) for collecting and archiving the IPCC/AR4 model data, the JSC/CLIVAR Working Groups on Coupled Modeling (WGCM) and their Coupled Model Intercomparison Project (CMIP) and Climate Simulation Panel for organizing the model data analysis activity, and the IPCC WG1 TSU for technical support. The IPCC Data Archive at Lawrence Livermore National Laboratory is supported by the Office of Sciences, U.S. Department of Energy. This work is supported, in part, by a grant from the U.S. National Science Foundation to Columbia University and a McGill start-up fund.

References

- Arblaster, J. M., and G. A. Meehl (2006), Contribution of external forcings to Southern Annular Mode trends, *J. Clim.*, **19**, 2896–2905.
- Cai, W., and T. Cowan (2007), Trends in Southern Hemisphere circulation in IPCC AR4 models over 1950–99: Ozone depletion versus greenhouse forcing, *J. Clim.*, **20**, 681–693.
- Eyring, V., et al. (2007), Multimodel projections of stratospheric ozone in the 21st century, *J. Geophys. Res.*, **112**, D16303, doi:10.1029/2006JD008332.
- Gillett, N. P., and D. W. J. Thompson (2003), Simulation of recent Southern Hemisphere climate change, *Science*, **302**, 273–275.

- Hu, Y., and Q. Fu (2007), Observed poleward expansion of the Hadley circulation since 1979, *Atmos. Chem. Phys.*, **7**, 5229–5236.
- Karpechko, A. Yu., N. P. Gillett, G. J. Marshall, and A. A. Scaife (2008), Stratospheric influence on circulation changes in the Southern Hemisphere troposphere in coupled climate models, *Geophys. Res. Lett.*, **35**, L20806, doi:10.1029/2008GL035354.
- Lorenz, D. J., and E. T. DeWeaver (2007), Tropopause height and zonal wind response to global warming in the IPCC scenario integrations, *J. Geophys. Res.*, **112**, D10119, doi:10.1029/2006JD008087.
- Lu, J., G. Chen, and D. M. W. Frierson (2008), Response of the zonal mean atmospheric circulation to El Niño versus global warming, *J. Clim.*, **22**, 5835–5851.
- Marshall, G. J. (2003), Trends in the Southern Annular Mode from observations and reanalyses, *J. Clim.*, **16**, 4134–4143.
- Meehl, G. A., C. Covey, T. Delworth, M. Latif, B. McAvaney, J. F. B. Mitchell, R. J. Stouffer, and K. E. Taylor (2007), The WCRP CMIP3 multimodel dataset, *Bull. Am. Meteorol. Soc.*, **88**, 1383–1394.
- Miller, R. L., G. A. Schmidt, and D. T. Shindell (2006), Forced annular variations in the 20th century Intergovernmental Panel on Climate Change Fourth Assessment Report models, *J. Geophys. Res.*, **111**, D18101, doi:10.1029/2005JD006323.
- Polvani, L. M., and P. J. Kushner (2002), Tropospheric response to stratospheric perturbations in a relatively simple general circulation model, *Geophys. Res. Lett.*, **29**(7), 1114, doi:10.1029/2001GL014284.
- Shindell, D. T., and G. A. Schmidt (2004), Southern Hemisphere climate response to ozone changes and greenhouse gas increases, *Geophys. Res. Lett.*, **31**, L18209, doi:10.1029/2004GL020724.
- Son, S.-W., et al. (2008), The impact of stratospheric ozone recovery on the Southern Hemisphere westerly jet, *Science*, **320**, 1486–1489.
- Son, S.-W., L. M. Polvani, D. W. Waugh, T. Birner, H. Akiyoshi, R. R. Garcia, A. Gettelman, D. A. Plummer, and E. Rozanov (2009), The impact of stratospheric ozone recovery on tropopause height trends, *J. Clim.*, **22**, 429–445.
- Steig, E. J., D. P. Schneider, S. D. Rutherford, M. E. Mann, J. C. Comiso, and D. T. Shindell (2009), Warming of the Antarctic ice-sheet surface since the 1957 International Geophysical Year, *Nature*, **457**, 459–462.
- Thompson, D. W. J., and S. Solomon (2002), Interpretation of recent Southern Hemisphere climate change, *Science*, **296**, 895–899.
- Thompson, D. W. J., J. M. Wallace, and G. C. Hegerl (2000), Annular modes in the extratropical circulation. Part II: Trends, *J. Clim.*, **13**, 1018–1036.
- Yin, J. H. (2005), A consistent poleward shift of the storm tracks in simulations of 21st century climate, *Geophys. Res. Lett.*, **32**, L18701, doi:10.1029/2005GL023684.

L. M. Polvani and N. F. Tandon, Department of Applied Physics and Applied Mathematics, Columbia University, 500 West 120th Street, New York, NY 10027, USA.

S.-W. Son, Department of Atmospheric and Oceanic Sciences, McGill University, 805 Sherbrooke Street West, Montreal, QC H3A 2K6, Canada. (seok-woo.son@mcgill.ca)

D. W. Waugh, Department of Earth and Planetary Sciences, Johns Hopkins University, Baltimore, MD 21218, USA.